

 Open access • Journal Article • DOI:10.1039/C8TC00175H

Thermally activated delayed fluorescence with a narrow emission spectrum and organic room temperature phosphorescence by controlling spin–orbit coupling and phosphorescence lifetime of metal-free organic molecules — [Source link](#)

Piotr Pander, Agnieszka Swist, Radoslaw Motyka, Jadwiga Sołoducho ...+4 more authors

Institutions: Durham University, Wrocław University of Technology, Silesian University of Technology, Polish Academy of Sciences

Published on: 24 May 2018 - Journal of Materials Chemistry C (The Royal Society of Chemistry)

Topics: Phosphorescence and Common emitter

Related papers:

- [Highly efficient organic light-emitting diodes from delayed fluorescence](#)
- [Synthesis, photophysical and electrochemical studies of acridone-amine based donor–acceptors for hole transport materials](#)
- [Purely Organic Thermally Activated Delayed Fluorescence Materials for Organic Light-Emitting Diodes.](#)
- [Thermally Activated Delayed Fluorescence \(Green\) in Undoped Film and Exciplex Emission \(Blue\) in Acridone–Carbazole Derivatives for OLEDs](#)
- [Acridinone/amine\(carbazole\)-based bipolar molecules: efficient hosts for fluorescent and phosphorescent emitters.](#)

Share this paper:    

View more about this paper here: <https://typeset.io/papers/thermally-activated-delayed-fluorescence-with-a-narrow-3rxi53cao3>

Durham Research Online

Deposited in DRO:

09 May 2018

Version of attached file:

Accepted Version

Peer-review status of attached file:

Peer-reviewed

Citation for published item:

Pander, Piotr Henryk and Swist, Agnieszka and Soloducho, Jadwiga and Dias, Fernando and Data, Przemyslaw (2018) 'Thermally activated delayed fluorescence with narrow emission spectrum and organic room temperature phosphorescence by controlling spin-orbit coupling and phosphorescence lifetime of metal-free organic molecules.', *Journal of materials chemistry C.*, 6 (20). 5434–5443.

Further information on publisher's website:

<https://doi.org/10.1039/C8TC00175H>

Publisher's copyright statement:

Additional information:

Use policy

The full-text may be used and/or reproduced, and given to third parties in any format or medium, without prior permission or charge, for personal research or study, educational, or not-for-profit purposes provided that:

- a full bibliographic reference is made to the original source
- a [link](#) is made to the metadata record in DRO
- the full-text is not changed in any way

The full-text must not be sold in any format or medium without the formal permission of the copyright holders.

Please consult the [full DRO policy](#) for further details.

Journal of Materials Chemistry C

Accepted Manuscript



This article can be cited before page numbers have been issued, to do this please use: P. H. Pander, A. Swist, J. Soloducho, F. Dias and P. Data, *J. Mater. Chem. C*, 2018, DOI: 10.1039/C8TC00175H.



This is an Accepted Manuscript, which has been through the Royal Society of Chemistry peer review process and has been accepted for publication.

Accepted Manuscripts are published online shortly after acceptance, before technical editing, formatting and proof reading. Using this free service, authors can make their results available to the community, in citable form, before we publish the edited article. We will replace this Accepted Manuscript with the edited and formatted Advance Article as soon as it is available.

You can find more information about Accepted Manuscripts in the [author guidelines](#).

Please note that technical editing may introduce minor changes to the text and/or graphics, which may alter content. The journal's standard [Terms & Conditions](#) and the ethical guidelines, outlined in our [author and reviewer resource centre](#), still apply. In no event shall the Royal Society of Chemistry be held responsible for any errors or omissions in this Accepted Manuscript or any consequences arising from the use of any information it contains.

ARTICLE

Thermally Activated Delayed Fluorescence with Narrow Emission Spectrum and Organic Room Temperature Phosphorescence by Controlling Spin-Orbit Coupling and Phosphorescence Lifetime of Metal-Free Organic Molecules†

Received 00th January 20xx,
Accepted 00th January 20xx

DOI: 10.1039/x0xx00000x

www.rsc.org/

Piotr Pander,^a Agnieszka Swist,^b Radoslaw Motyka,^c Jadwiga Soloduch,^b Fernando B. Dias,^a Przemyslaw Data^{*a,c,d}

This work presents a study of two organic molecules with very similar, large singlet-triplet energy gap, of which one is a thermally activated delayed fluorescence (TADF) emitter and the other a room temperature phosphorescence (RTP) emitter. By investigating their photophysical properties we are able to explain their distinct behavior. The molecules are studied in non-polar polymer and OLED hosts. Furthermore, this work presents a CT TADF emitter that shows narrow and resolved electroluminescence spectrum (FWHM = 53 nm). The study shows efficient RTP emitter based on a D-D-D structure and also a first acridone-based TADF emitter with a D-A-D structure.

Introduction

Acridones have been known as biologically active compounds^{1–4}, however recently they are used as electron-accepting units of several donor-acceptor and donor-acceptor-donor systems.^{5–7} The acridone moiety is very special because it contains an electron-accepting carbonyl group (>C=O) along with an electron-donating nitrogen atom bearing a lone electron pair. Acridone as a commercially available⁸ building block is a good candidate to use as a cheap and commonly available acceptor in OLED emitters.⁹ On the other hand, phenothiazine is very popular in drug applications, i.e. in chlorpromazine.¹⁰ Phenothiazine and carbazole, however, among others, have recently become popular as donors in donor-acceptor molecules, such as TADF emitters.^{11–14}

Thermally activated delayed fluorescent (TADF) OLED materials have been widely investigated in recent years by several groups around the globe.^{15–28} In the simplest way, TADF or E-type^{19,29} delayed fluorescence is a long-lived photoluminescence which originates through reverse intersystem crossing (rISC) mechanism from the lowest triplet (T_1) to the lowest singlet state (S_1), directly or through a mediator state,³⁰ which enables to harvest up to 100% of triplet states.^{18,19} TADF is therefore

crucial in OLED devices since 75% of excited states formed as a result of charge recombination are triplets.^{11,15,31} Previous approaches in efficient triplet state harvesting involved phosphorescent heavy metal complexes.^{29–31} A typical TADF emitter does not contain rare precious metals, however, metal-based TADF emitters, such as copper complexes have also been widely investigated over recent years.^{34–37} On the other hand, almost all TADF emitters are donor-acceptor type structures

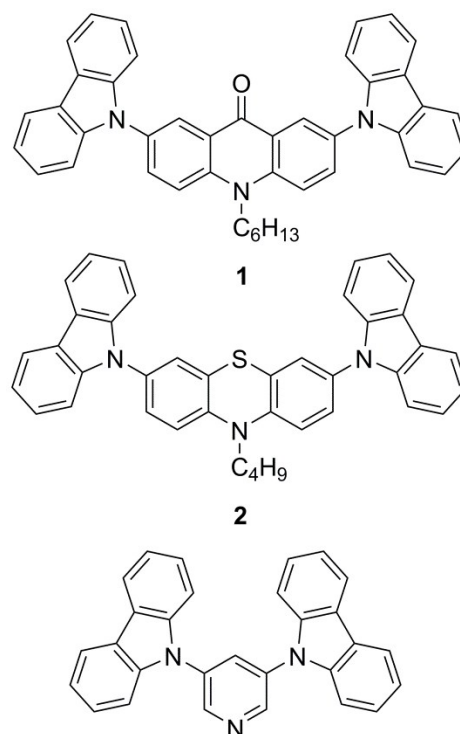


Chart 1 Investigated molecules.

^a Department of Physics, Durham University, South Road, Durham, DH1 3LE, United Kingdom. E-mail: Przemyslaw.*Email - Data@dur.ac.uk

^b Faculty of Chemistry, Wrocław University of Technology, Wybrzeże Wyspińskiego 27, 50-370 Wrocław, Poland

^c Faculty of Chemistry, Silesian University of Technology, Ks. M. Strzody 9, 44-100 Gliwice, Poland

^d Centre of Polymer and Carbon Materials, Polish Academy of Sciences, M. Curie-Skłodowskiej 34, 41-819 Zabrze, Poland

† Electronic Supplementary Information (ESI) available: experimental details, additional photophysics results. See DOI: 10.1039/x0xx00000x

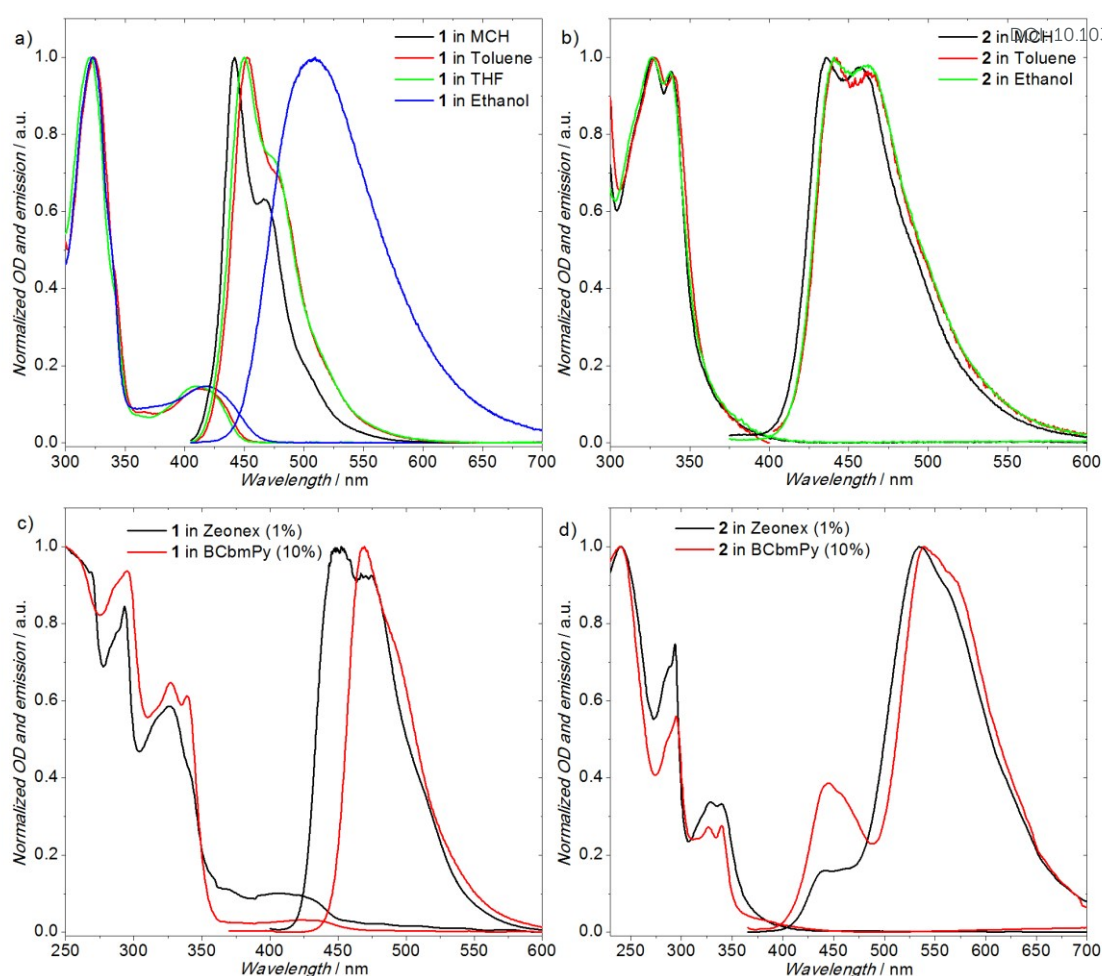


Figure 1 Photoluminescence and absorption spectra of **1** and **2** in various solvents and matrices: a), b) UV-Vis and fluorescence spectra in solution; c), d) UV-Vis and fluorescence spectra in solid films.

showing broad charge transfer (CT) emission. TADF does not require CT states, but the use of CT states is a very simple way to decrease singlet-triplet energy gap. This negatively impacts color purity of OLED electroluminescence as the emission of those molecules is broad, with large full width at half maximum (FWHM). Using donor-acceptor molecules with weak CT character may result in materials showing narrow, resolved emission even in the OLED host, but still being able to harvest triplets. It is worth to point out that not only TADF emitters may supersede metal complexes in OLED applications, as also metal-free organic room temperature phosphors show a promising perspective for their future application in the field.^{38–41} Metal-free organic phosphors show a substantial triplet formation yield along with a relatively fast triplet radiative decay, similarly to metal complexes, but without heavy metal content. If non-radiative decay is successfully suppressed, the organic phosphors can exhibit long-lived emission.^{41,42} In this work, we present the first TADF emitter which uses acridone as an acceptor in the D-A-D configuration. Moreover, a high triplet molecule **BCbmPy** has been used as a host material. The properties of D-A-D TADF system **1** with D-D-D RTP molecule **2** are compared using photophysical approach and in OLED devices. Comparing these molecules gives an insight into

the understanding of the similarities and dissimilarities between TADF and RTP emitters.

Results and discussion

Steady-state photophysics

Starting from the basic photophysical behavior of molecules, the presented systems are investigated in solution. In **1** four absorption bands can be observed in methylcyclohexane (MCH) solution (**Figure S3** in supporting information): $\lambda_{\max} = 239$ nm ($\epsilon \approx 9 \cdot 10^4$ M⁻¹ cm⁻¹), $\lambda_{\max} = 291$ nm ($\epsilon \approx 4 \cdot 10^4$ M⁻¹ cm⁻¹), $\lambda_{\max} = 322$ nm ($\epsilon \approx 3 \cdot 10^4$ M⁻¹ cm⁻¹), $\lambda_{\max} = 407$ nm ($\epsilon \approx 5 \cdot 10^3$ M⁻¹ cm⁻¹). The three first absorption bands are associated with π - π^* transitions due to their high absorption coefficients. The fourth $\lambda_{\max} = 407$ nm is associated with a transition forbidden by geometry, such as CT, due to a small absorption coefficient. Series of absorption spectra recorded in solvents of different polarity show that this low-energy absorption band red-shifts upon increasing dielectric constant of the solvent (**Figure 1**). Band maximum shifts from 407 nm in MCH to 418 nm in ethanol, whereas *onset* shifts from 445 nm to 465 nm, respectively. This is a typical behavior for a charge-transfer absorption band, where an excited state with large dipole moment is stabilized by

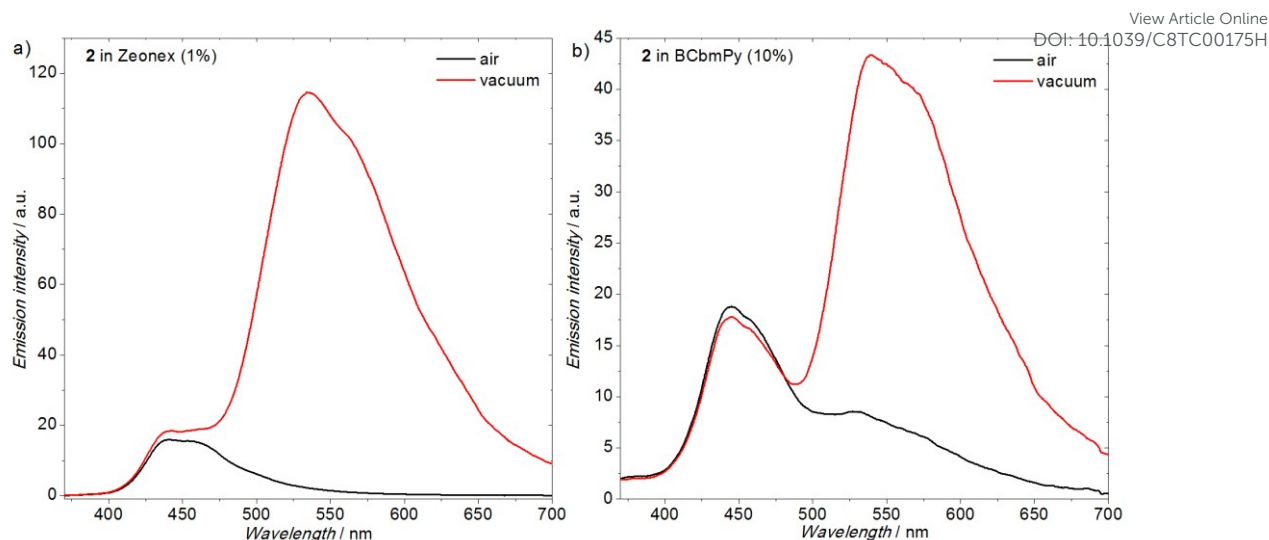


Figure 2 Steady-state photoluminescence spectra of **2** doped in Zeonex (drop-cast) and **BCbmPy** (coevaporation) recorded in air and in a vacuum.

molecules of polar solvent. Interestingly, only one absorption band, $\lambda_{\max} = 291$ nm can clearly be attributed to carbazole moiety, whereas none of the unsubstituted acridone⁷ absorption bands can be directly found in **1** absorption spectrum. However, the absorption bands related to each subunit of **1** can be indicated using literature data⁴³ and by comparison with the absorption spectrum of compound **2** (Figure S3). The emission of **1** is clearly resolved in methylcyclohexane, toluene, and tetrahydrofuran, but in ethanol, the fluorescence spectrum is broad and featureless (Figure 1a). The lowest excited state in **1** has a weak charge transfer character. The fluorescence spectrum remains resolved in non-polar or moderately-polar solvents, where charge separation is small (i.e. producing a hybrid local and charge transfer state, CT + LE, or so-called weak CT). Highly polar solvent, such as ethanol, promotes charge separation, giving rise to a typical broad CT emission. This is consistent with previous, calculation-based observations of a hybrid local and charge transfer character of HOMO-LUMO transition in **1**.⁴⁴

Absorption bands of **2** in MCH (Figure S3) are: $\lambda_{\max} = 238$ nm ($\epsilon \approx 8 \cdot 10^4$ M⁻¹ cm⁻¹), $\lambda_{\max} = 292$ nm ($\epsilon \approx 5 \cdot 10^4$ M⁻¹ cm⁻¹), characteristic absorption band of carbazole with two maxima $\lambda_{\max} = 326, 338$ nm ($\epsilon \approx 1.5 \cdot 10^4$ M⁻¹ cm⁻¹), and a shoulder $\lambda_{\text{sh}} = 345\text{-}407$ nm ($\epsilon < 8 \cdot 10^3$ M⁻¹ cm⁻¹). The first two absorption bands have the same origin as respective absorption bands in **1** and should, therefore, be attributed to $\pi\text{-}\pi^*$ transitions, whereas the latter is a shoulder of the $n\text{-}\pi^*$ transition in phenothiazine. The emission spectrum of **2**, which shows blue fluorescence, hardly changes with solvent polarity, suggesting no involvement of charge transfer states. Such a behavior is a result of its D-D-D structure where neither carbazole nor phenothiazine show pronounced acceptor properties.

In fact, both compounds show blue fluorescence in diluted toluene solution. Interestingly, they show significantly different photoluminescence quantum yield (PLQY). PLQY of a degassed toluene solution of **1** ($\Phi_{\text{PL}} = 0.79$) is much larger than the value obtained for **2** ($\Phi_{\text{PL}} = 0.05$). Phenothiazine moiety induces high

triplet formation yield in **2** which therefore leads to a low Φ_{PL} in solution. Interestingly, photoluminescence of **2** doped in polymer films in the presence of air is very similar to a toluene solution ($\Phi_{\text{PL}} = 0.05$). However, in a vacuum, the emission spectrum reveals additional band which in turn causes a rise in the photoluminescence quantum yield ($\Phi_{\text{PL}} = 0.58$) (Figure 2). Oxygen normally quenches long-lived triplet states, therefore the difference in photoluminescence between air and vacuum is due to long-lived emission from a triplet state, such as phosphorescence.

A typical TADF emitter with a D-A-D structure usually shows featureless, pure CT emission when dispersed in OLED matrix¹⁷⁻²³. However, **1** shows a narrow, resolved photoluminescence in the OLED host (Figure 1c), suggesting a mixed CT + LE nature of the emissive state. The full width at half maximum FWHM = 54 nm, is among the smallest values for TADF molecules. In fact, identical FWHM and spectrum are observed in electroluminescence (Figure 6a, Dev 1). It is worth to note that comparably small FWHM values are only observed for deep blue emission, i.e. FWHM = 46 nm.⁴⁵ Seemingly narrow spectra of deep blue emitters are due to the properties of nanometer wavelength scale which causes the spectra in blue to appear narrower and in red to be broader. To avoid this effect the emission spectra should be presented in cm⁻¹ or eV which would be more practical in comparing different color emissions (such as blue and red). Unfortunately, FWHM values used to be given in nanometers. In the light of that conclusion, it is stated that FWHM of 54 nm is extremely low in comparison with typical values observed in the range of sky-blue TADF emitters. This typically varies in the range of 100-150 nm.⁴⁶⁻⁴⁹ Low value of FWHM is important for the color purity of emission in practical applications, such as in Samsung Galaxy cell phones.⁵⁰ It is worth to note that some recently developed TADF emitters, exploiting B-N multiple resonance effect⁵⁰ shows much narrower emission with FWHM = 28 nm. However, those emitters exhibit a completely different molecular design than the molecule presented here, thus, in fact, they do not present any CT

properties. It is worth to note that although the devices showed high EQE of 20.2% the maximum brightness obtained was

the presence of air. More intense phosphorescence than in **BCbmPy** is observed in zeonex due to a better suppression of

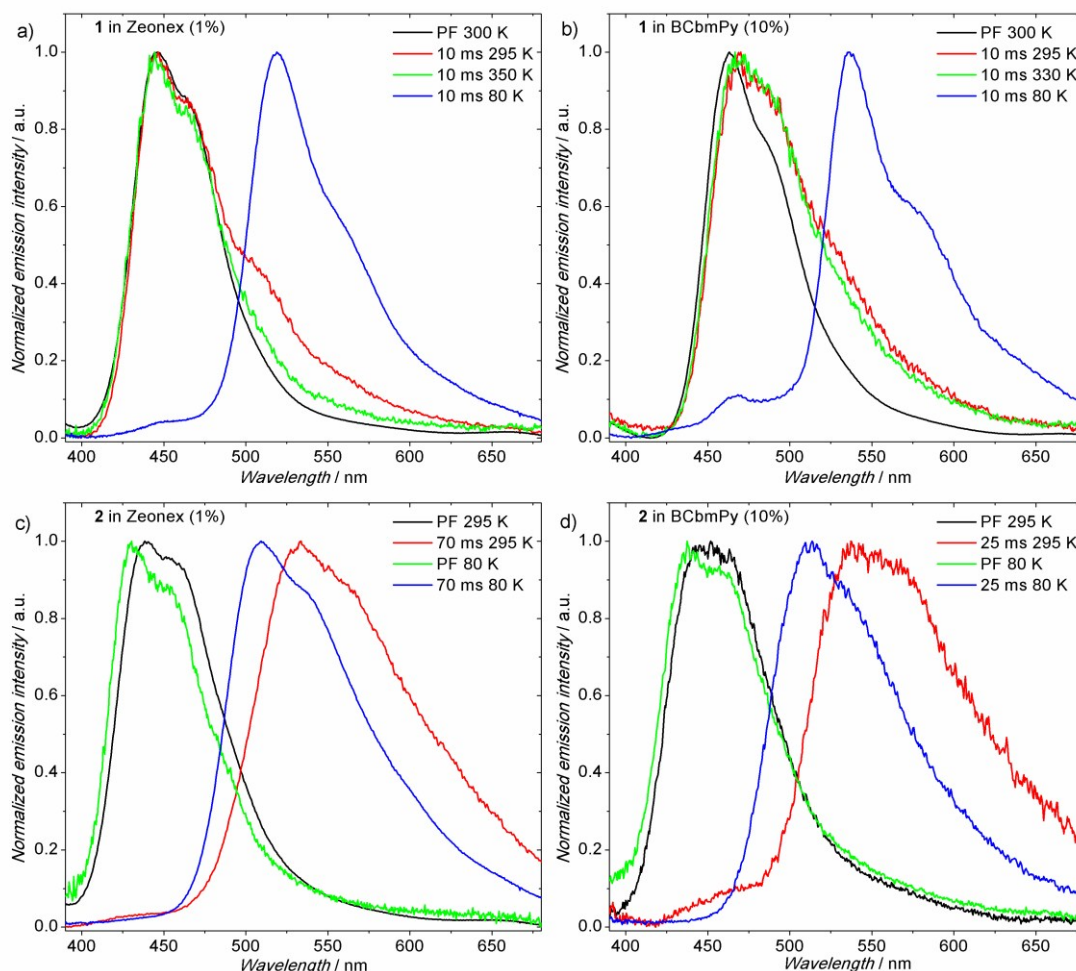


Figure 3 Time-resolved photoluminescence spectra of the molecules doped into Zeonex and **BCbmPy**.

extremely low, the OLEDs have also shown a significant roll-off. Compound **1** shows similar, narrow photoluminescence spectrum shape in toluene, zeonex and OLED host, this means **1** is not significantly susceptible to the polarity/polarizability of the environment which is due to its weak CT nature. However, **1** shows a bathochromic shift in OLED host respective to toluene and zeonex. In toluene solution or zeonex **1** shows blue fluorescence with a maximum at ≈ 450 nm, while the emission in **BCbmPy** is red shifted with a maximum at ≈ 470 nm. Note the reasons for the redshift are given later in the text. To conclude, only a strongly polar medium, such as ethanol, can stabilize the charge transfer state in this molecule to give a broad, featureless emission spectrum.

As mentioned previously, molecule **2** is a room temperature phosphor (Figure 2). The phosphorescence of molecule **2** is so strong it constitutes 91 % of total emission in zeonex and over 60 % in **BCbmPy**, at room temperature. This suggests that triplet formation yield of **2** is very high as for a metal-free molecule. It is worth to note that due to relatively low oxygen permeability of **BCbmPy** there is a trace of phosphorescence visible also in

non-radiative decay in the polymer film.

Time-resolved photoluminescence study

Time-resolved spectra of **1** in the solid state (Figure 3a,b) stay in agreement with the steady-state spectra presented above. Prompt and delayed fluorescence in the zeonex overlap. Note there is not only TADF observable, but RTP is present too and forms a shoulder on the red edge of the spectrum. No changes to the prompt and delayed fluorescence spectra in function of time can be observed therefore the system is rather not complicated to describe. Singlet $S_1 = 2.96$ eV and triplet $T_1 = 2.54$ eV energy can be derived from prompt fluorescence and phosphorescence onsets. From these values, a large singlet-triplet splitting $\Delta E_{S-T} = 0.42$ eV is calculated. **1** doped in **BCbmPy** exhibits more complicated photophysical behavior. The prompt and delayed fluorescence spectra do not overlap perfectly. This suggests that prompt and delayed fluorescence originates from molecules with different surrounding or conformation. Most probably, delayed fluorescence originates from relaxed molecules, whereas prompt fluorescence originates from non-

relaxed molecules (also see **Figure S2b** in supporting information). Other observations are rather similar to the effects present in zeonex. Also here an insignificant contribution of room temperature phosphorescence is observed. Interestingly, even at temperatures as low as 80 K, there is still a small portion of delayed fluorescence present as a shoulder between 450-500 nm (**Figure 3b**). Laser fluence experiment (**Figure S2a**) indicates clearly a supralinear power dependence, therefore this emission can be attributed mostly to triplet-triplet annihilation (TTA). It is clear that at higher doping concentrations (such as 10% in the solid film) molecules are relatively close to each other and are able to diffuse and collide even at low temperature. Such interaction of two molecules in triplet state leads to triplet fusion.

Phosphorescence spectra of **1** observed in zeonex and in **BCbmPy** show identical vibronic structure (**Figure 3a, 3b**). Interestingly, the triplet emission in the host is visibly red-shifted, resulting in a lower triplet energy of **1** in **BCbmPy** than in zeonex. Both singlet $S_1 = 2.83$ eV and triplet $T_1 = 2.43$ eV energy in **BCbmPy** doped film is shifted by almost the same value, relative to zeonex, resulting in nearly identical $\Delta E_{S-T} = 0.40$ eV as in zeonex. A simultaneous decrease in S_1 and T_1 energy in

BCbmPy is related most likely with a π - π interaction between the host and the dopant. It affects both the triplet and the singlet as both bears a partially delocalized character. This interaction is not present in zeonex as the polymer is fully aliphatic. Taking into account experimental errors for determination of singlet-triplet gaps, usually in a range of ± 0.03 - 0.05 eV, the two singlet-triplet energy gaps (in zeonex and **BCbmPy**) can be considered as identical within the margin of error. Presence of both RTP and TADF is due to a large singlet-triplet energy gap of this material $\Delta E_{ST} \approx 0.4$ eV. Reverse intersystem crossing (rISC) is not fast enough to efficiently harvest all triplet states by the way of TADF, therefore a small population of molecules relaxes radiatively from the triplet state, emitting phosphorescence.

Time-resolved spectra of **2** dispersed in Zeonex (**Figure 3c,d**) show the energy of singlet $S_1 = 3.02$ eV and triplet $T_1 = 2.56$ eV states to be close to the respective values observed in **1**. Moreover, the singlet-triplet energy splitting is also similar, $\Delta E_{S-T} = 0.46$ eV. It is worth to note that in both hosts (zeonex and **BCbmPy**) the phosphorescence of **2** is blue-shifted at low temperature. This suggests that **2** shows rigidochromism. The molecular motion causing this effect is considered to be related

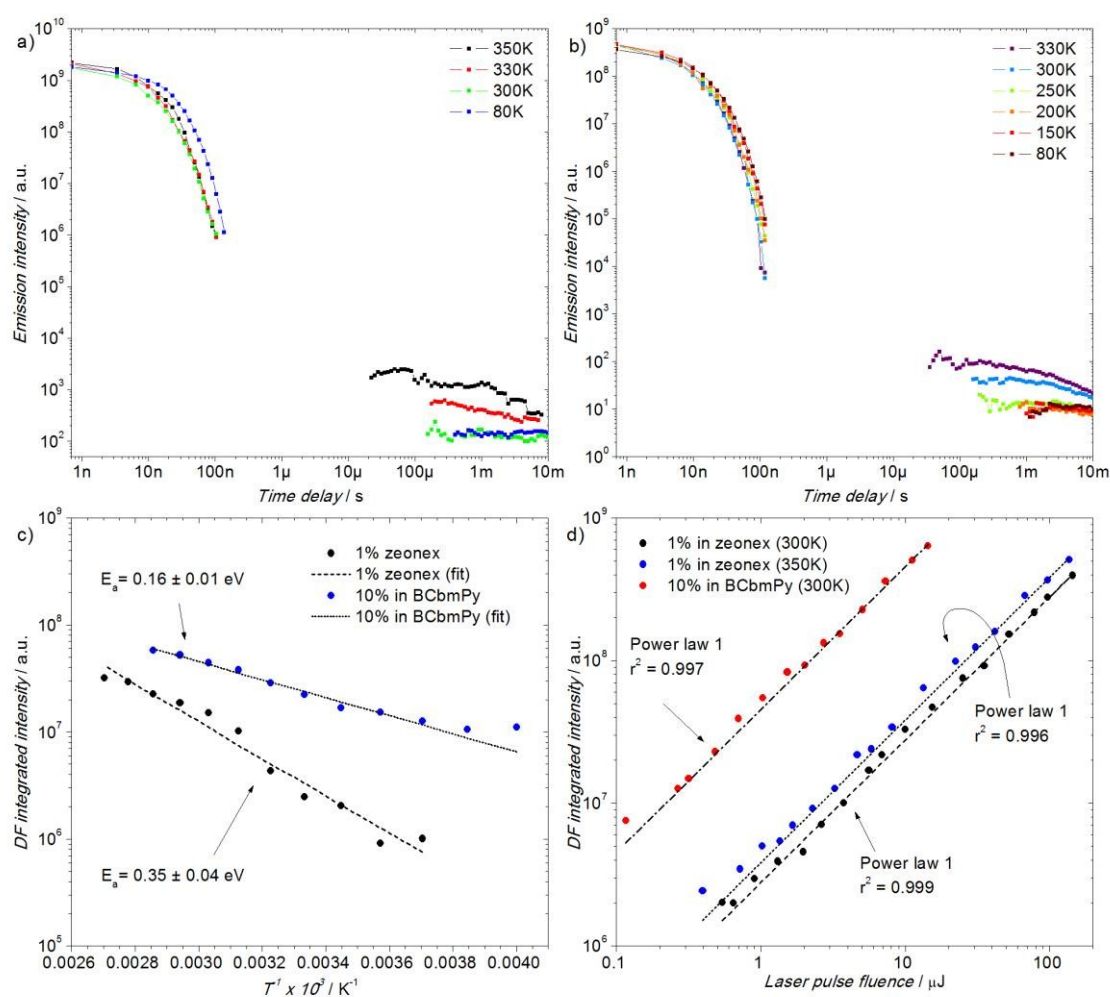


Figure 4 a), b) Photoluminescence decay of **1** at various temperatures; c) d) Power and temperature dependence of **1** emission in zeonex and **BCbmPy**.

with fast interconversion between *H*-intra and *H*-extra like conformers of phenothiazine or with the thermal oscillation of the most stable conformer.^{13,20,51–53} It has been observed that the existence of these two conformers sometimes affects molecules photophysical behavior,^{13,20,53} however in unhindered phenothiazines this is unlikely due to a small energy barrier for the interconversion.⁵² Having this established we argue that in **2**, the *N*-*n*-butyl group causes insignificant steric hindrance, insufficient to pose any energy barrier large enough to obstruct the *H*-intra / *H*-extra interconversion. In such a situation the high energy conformer is quickly interconverted to the most stable counterpart and thus only one ground state conformer is observed in the photophysics. Knowing all these results presented above it is not clear why does **1** show TADF whereas **2** does not? Why in **1** the phosphorescence at room temperature is very weak, but in **2** it is much stronger than fluorescence? Why is there any TADF in **1** at all? One can say the reason is the difference of the nature of respective emissive states: **1** is a CT+LE emitter while **2** a $\pi\pi^*$ emitter. In **1** the CT+LE singlet is coupled with a partially delocalized $^3\pi\pi^*$ state located on acridone giving optimal conditions for rISC, except for large ΔE_{S-T} . In **2** the triplet state is located on phenothiazine moiety as literature data suggests (i.e. carbazole triplet is located at ca. 3 eV).^{54,55} The phosphorescence of **2** is also very similar in energy and spectrum shape to the phosphorescence of phenothiazine itself¹², however slightly red-shifted. We assign the red-shift to the effect of substitution with carbazole units. This causes similar, partial delocalization of the triplet state as in molecule **1** (described below). It can be concluded from the steady-state spectra (Figure 1b and 1d) that the singlet state in **2** has a major $\pi\pi^*$ character. On the other hand the triplet state, as short-lived, has $\pi\pi^*$ character too. Obviously, a direct transition between $^1\pi\pi^*$ and $^3\pi\pi^*$ should be very slow due to their similar geometry, therefore there must be at least one upper $^3\pi\pi^*$ state which acts as an intermediate energy level to explain fast intersystem crossing in **2**. A potential candidate for such a state

configuration for a TADF emitter (i.e. no CT states), however, high phosphorescence intensity and low fluorescence quantum yield suggest strong spin-orbit coupling and relatively fast intersystem crossing (ISC). rISC and ISC represent in fact the same spin-flip process, which only proceeds in a different direction. Therefore, if ISC is fast, rISC should be too. However, rISC rate constant, as for an endothermic process is limited by Arrhenius relation. For this reason, rISC is slower than ISC at room temperature.

In terms of possible TADF properties of the molecule its general structural concept, such as D-A-D or D-D-D structure is irrelevant. It is only much easier to design a donor-acceptor TADF emitter than any other. TADF properties have been found in numerous molecules without D-A or D-A-D structure and without CT states, including D-D-D systems.^{24,56–58}

Prompt fluorescence of **1** is very strong and relatively long-lived which suggests slow ISC. Large singlet-triplet splitting, on the other hand, implies slow rISC, in fact, delayed fluorescence lifetime reaches 26 ms in zeonex (Table 1). This value is surprisingly comparable with the RTP lifetime of **2** which is 22 ms. Speaking about RTP and TADF lifetimes at room temperature it is important to also note phosphorescence lifetime at low temperature (i.e. 80 K) to observe the effects of reduced thermal energy and suppression of non-radiative decay. Phosphorescence lifetime of **1** at 80 K is significantly longer than 100 ms (0.5 ± 0.2 s). On the other hand, phosphorescence lifetime of **2** increases only to 38 ms. From these observations, we conclude the triplet state of **1** has a long lifetime and as such promotes TADF. This is because a long-lived triplet state gives enough time for rISC to take place. On the other hand, **2** shows a short phosphorescence lifetime, even at 80 K, which indicates the triplet lives short due to the relatively large radiative rate constant. This clearly quenches TADF as due to a large $\Delta E_{S-T} = 0.46$ eV the rISC rate is too slow. The results show the lowest $^3\pi\pi^*$ triplet state is more suitable for TADF emitter than $^3\pi\pi^*$ if the ΔE_{S-T} is large.

The data presented in this work enable to explain either why **1**

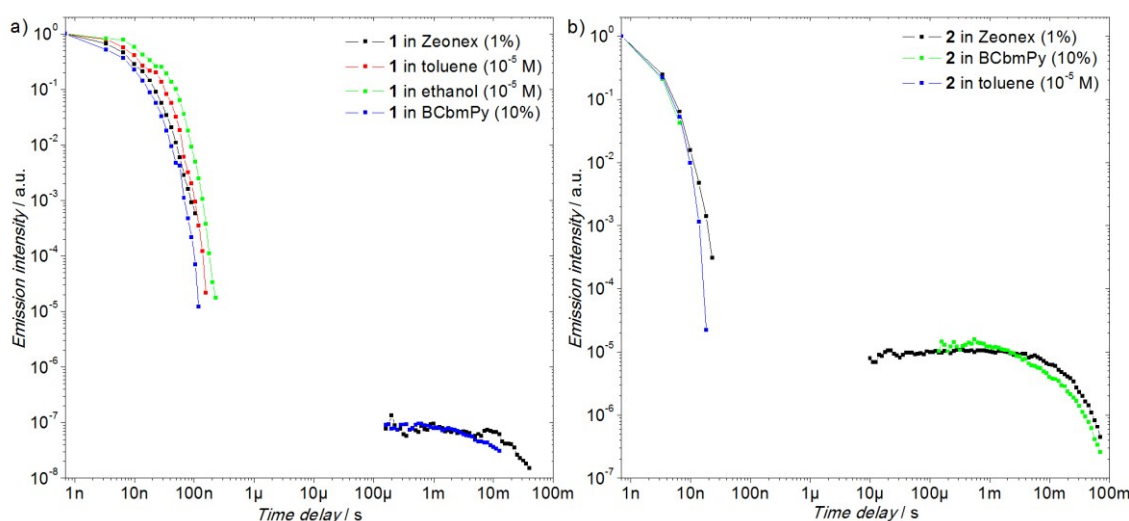


Figure 5 Photoluminescence decay of **1** and **2** in various matrices and solvents at room temperature.

is carbazole $^3\pi\pi^*$ local triplet state. This is not a typical is a TADF emitter and why **2** is not and shows RTP properties

instead. It is concluded that TADF emitters with wide energy gap, like **1** must exhibit long phosphorescence lifetime, which is significantly longer than TADF lifetime at room temperature. On the other hand, short phosphorescence lifetime at room temperature kills TADF as efficient rISC in these conditions is impossible. The observations, however, seem obvious, are rarely taken into account. As TADF and RTP are in fact two sides of the same coin it is not only the ΔE_{S-T} which makes the material a TADF emitter or not. A lifetime of the triplet state at room temperature, in fact, is also very important. What really decides on the properties of the molecule is the relation of the rISC rate constant to the lowest triplet state lifetime (including both radiative and non-radiative decay). Long triplet state lifetime promotes TADF while short quenches it. Usually, a short triplet lifetime is caused by non-radiative decay. In this situation, the molecule is only a fluorescent emitter. If the short triplet lifetime is due to a fast radiative decay then RTP is observed as is in **2**. All emitters with sufficient phosphorescence lifetime in relation to the ΔE_{S-T} will present TADF properties, regardless of their structure.

It has been observed that phosphorescence spectrum of D-A or D-A-D molecules with limited D-A conjugation is identical or very similar to the phosphorescence spectrum of donor or acceptor.^{12,23,59} However, in some cases the phosphorescence of such a molecule is red-shifted or distorted in relation to the phosphorescence of the donor or acceptor due to the effect of partial conjugation.^{23,60} Carbazole phosphorescence has already been described in literature^{54,55} and its triplet level energy is roughly equal to 3 eV. Moreover, the vibronic structure of carbazole phosphorescence spectrum is different from that observed in **1** (Figure 3a, 3b). On the other hand, phosphorescence of *N*-substituted acridone-containing molecules⁶ has a similar vibronic structure to the spectrum reported in this work. The triplet energy of those molecules is higher (2.8 eV) than in the case presented here (2.54 eV). In **1** the electron-donating carbazole moieties red-shift acridone phosphorescence spectrum (decrease triplet state energy) by conjugating with the central acridone unit. The impact of *C*-substitution, so extended conjugation, on acridone is also

observed in absorption spectra. Absorption bands of unsubstituted and 2,6-substituted⁷ acridone derivatives are completely different and characteristic absorption bands seen in unsubstituted acridone are not visible in the spectra of the derivatives. This shows that 2,6-substituted acridone, with carbazole (this work) or diphenylamine⁷, is partially conjugated with the attached donor moieties.

Delayed fluorescence of **1** shows clear temperature dependence in both Zeonex and **BCbmPy** matrices (Figure 4a, b, c). Interestingly, the effect of temperature on the decay profile seems to be negligible below temperatures 300-250K. This behavior is caused by phosphorescence emission, which increases its intensity at low temperatures. Prompt fluorescence in either host is almost not affected by the temperature change. Lifetimes of prompt fluorescence in films are similar, close to 10 ns. But a lifetime of delayed fluorescence is remarkably long: ≈ 30 ms in Zeonex and ≈ 10 ms in the OLED host. This is also a result of a large singlet-triplet energy splitting. Power dependence of delayed fluorescence in both matrices is shown in Figure 4d. Linear dependence clearly shows that in both cases TADF mechanism is dominant at room temperature. Additionally, power dependence experiment was performed also at 350 K in the zeonex matrix, showing that the mechanism remains unchanged.

Temperature dependence of delayed fluorescence in **1** is especially interesting (Figure 4a,b,c). **1** in Zeonex shows TADF activation energy $E_a = 0.35 \pm 0.04$ eV which is within the experimental error identical to the value of ΔE_{ST} . Interestingly, **1** behaves differently in the **BCbmPy** host as the activation energy is reduced to only 0.16 ± 0.01 eV which is much lower than the $\Delta E_{ST} = 0.40$ eV recorded in this case. The reduced activation energy of **1** in **BCbmPy** explains high OLED EQE (Figure 6). The divergence between E_a and ΔE_{ST} , however typical, has not been fully explained yet. One possible explanation is a specific alignment of upper triplet states, which couple with both T_1 and S_1 , reducing the actual size of the energy barrier.¹⁹

Table 1 Spectroscopic properties of **1** and **2** in zeonex and toluene.

Compound	Matrix / solvent	λ_{abs} , nm ^a	λ_{em} , nm ^b	Φ_{PL} ^c	τ_{PF} , ns ^d	τ_{DF} , ms ^e	τ_{PH} , ms ^f	S_1 / T_1 , eV ^g	ΔE_{ST} , eV ^h
1	toluene	323, 413	469	0.79	14 ± 2	-	-	-	-
	zeonex	293, 326, 407	451	0.95	9.1 ± 0.6	26.8 ± 0.7	500 ± 200 (80 K)	2.96 / 2.54	0.42
2	toluene	327, 338	441, 462	0.05	1.81 ± 0.02	-	-	-	-
	zeonex	241, 294, 328, 340	439, 532	0.58	1.96 ± 0.02	-	23 ± 1 (295 K) 38 ± 2 (80 K)	3.02 / 2.56	0.46

^a Absorption maxima; ^b photoluminescence maxima; ^c Φ_{PL} photoluminescence quantum yield in specified solvent/ matrix in oxygen-free conditions; ^d prompt fluorescence lifetime; ^e delayed fluorescence lifetime; ^f phosphorescence lifetime; ^g singlet and triplet energy; ^h singlet-triplet energy splitting.

Photoluminescence decay of **1** and **2** is very similar in both zeonex and **BCbmPy**. However, **BCbmPy** reduces the E_a of the material **1**, so this improves its performance in the OLED host

relative to zeonex. Both hosts are relatively rigid, thus they effectively suppress non-radiative decay. Interestingly, delayed fluorescence in **1** and RTP in **2** can only be observed in solid

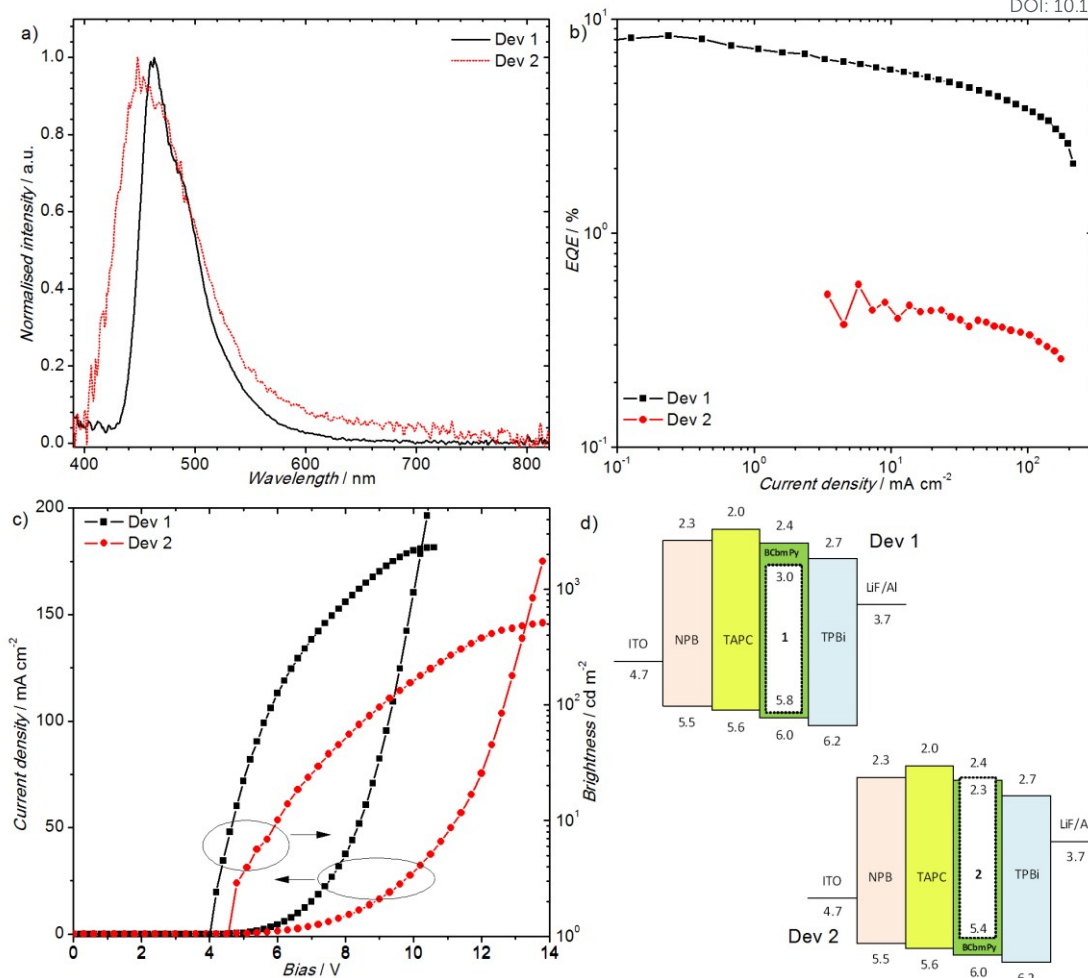


Figure 6 Characteristics of OLED devices fabricated using emitters and host presented in this work: a) electroluminescence spectra; b) EQE – current density characteristics; c) current density / brightness – voltage characteristics; d) schematic of device structures.

films (Figure 5a, 5b). In solutions, the emitter-solvent interactions, such as collisions, deactivate triplet state molecules, therefore no TADF, nor RTP can be observed. This is because the radiative lifetime of these molecules is very long, thus intermolecular collisions are able to quench long-lived triplet states before they undergo a radiative transition or rISC. The prompt fluorescence lifetime of **1** in toluene solution ($\tau = 14 \pm 2$ ns) is slightly larger than in solid state ($\tau \approx 9$ ns). Even longer lifetime $\tau = 18 \pm 2$ ns is observed in ethanol solution, where the emission has purely CT character.

On the other hand, **2** shows short-lived fluorescence both in zeonex and toluene (1.81 ± 0.02 ns and 1.96 ± 0.02 ns, respectively), which is due to a fast intersystem crossing. Phosphorescence of **2** in zeonex has a lifetime of only 23 ± 1 ms, which increases at 80 K to 38 ± 2 ms. Such a short phosphorescence lifetime confirms a strong $\pi\pi^*$ character of the triplet state and moderate spin-orbit coupling.

In both doped BCbmPy films weak triplet-triplet annihilation (TTA) is observed (Figures S2a, S5). This is likely associated with higher doping concentration in BCbmPy (10%) than in zeonex (1%) where this phenomenon does not appear. In **1** the TTA

emission in BCbmPy is observed only at low temperatures (Figure S2a).

OLED devices

OLED devices have been produced with the use of the materials presented (Figure 6). To confine the hole and electron ratio a structure ITO/NPB (40 nm)/TAPC (10 nm)/BCbmPy co 10% dopant (20 nm)/TPBi (60 nm)/LiF (1 nm)/Al(100 nm) has been used. The devices show to turn on voltage of 4 V (dopant **1**) and 4.6 V (dopant **2**) at 1 cd m⁻². The efficiency of devices is dictated by the Φ_{PL} of respective dopant. High EQE of 8.2% in Dev 1 is due to triplet harvesting by TADF mechanism. It is worth to note the narrow electroluminescence spectrum of Dev 1 with small FWHM = 53 nm. One of the smallest values among D-A or D-A-D TADF emitters. Dev 2, in fact, should also benefit from triplet harvesting in molecule **2**, at least by TTA or by the emission of phosphorescence. Unfortunately, the phosphorescence is not observed likely due to the presence of triplet-quenching processes, i.e. TTA or triplet-polaron annihilation. As a result, the maximal EQE of the device reaches only 0.5%. High triplet formation yield of **2** in the presence of triplet quenching

processes results in small EQE as all of the triplet states remain dark.

Conclusions

Two molecules with very similar and large ΔE_{ST} but absolutely different properties have been investigated. It was found that the reason for one being a TADF emitter and the other RTP emitter lies in the difference of their triplet lifetime. Therefore, triplet state lifetime is another effective factor determining a TADF emitter, apart from ΔE_{ST} . A TADF molecule must show triplet lifetime long enough so that with a given ΔE_{ST} rISC is faster than triplet decay, i.e. at room or higher temperature. RTP molecule **2** shows prominent phosphorescent properties with very high (90 %) phosphorescence contribution at room temperature.

OLED devices using both investigated molecules have been fabricated. The phosphorescent molecule **2** gave a device with 0.5 % EQE with only the fluorescence visible in electroluminescence spectrum. On the other hand, the TADF emitter **1** gave an efficient device with 8.2 % EQE and resolved, narrow electroluminescence with FWHM = 53 nm which is an exceptionally low value for a D-A or D-A-D TADF emitter. The device was also much brighter than the previously reported by Hatakeyama,⁵⁰ with FWHM = 28 nm, established by using multiple resonance effects in a TADF emitter. Design of new, efficient TADF emitters with narrow emission spectrum is an inevitable development pathway in the field, especially if the materials are meant to be used for display applications. This work presents a novel blue emitter with narrow electroluminescence spectrum and a new acridone acceptor which is used in D-A-D configuration for the first time to obtain TADF.

Conflicts of interest

There are no conflicts to declare.

Acknowledgments

P.P. thanks to the European Union for financial support from H2020-MSCA-ITN-2015 / 674990 EXCILIGHT grant. This work is financially supported by Polish National Science Centre, Project No.2012/05/B/ST5/00745.

Notes and references

- V. Nadaraj, S. Thamarai Selvi and S. Mohan, *Eur. J. Med. Chem.*, 2009, **44**, 976–980.
- J. P. Dheyongera, W. J. Geldenhuys, T. G. Dekker and C. J. Van der Schyf, *Bioorg. Med. Chem.*, 2005, **13**, 689–698.
- R. Hegde, P. Thimmaiah, M. C. Yerigeri, G. Krishnegowda, K. N. Thimmaiah and P. J. Houghton, *Eur. J. Med. Chem.*, 2004, **39**, 161–177.
- N. Bahr, E. Tierney, and J.-L. Reymond, *Tetrahedron Lett.*, 1997, **38**, 1489–1492.
- A. Świst, J. Cabaj, J. Soloducho, P. Data and M. Łapkowski, *Synth. Met.*, 2013, **180**, 1–8. DOI: 10.1039/C8TC00175H
- D. a K. Vezzu, J. C. Deaton, M. Shayeghi, Y. Li and S. Huo, *Org. Lett.*, 2009, **11**, 4310–4313.
- B. K. Sharma, A. M. Shaikh, N. Agarwal and R. M. Kamble, *RSC Adv.*, 2016, **6**, 17129–17137.
- 9(10H)-Acridanone, www.sigmaldrich.com/catalog/product/aldrich/150215, (accessed 10 January 2018).
- P. Data, A. Swist, M. Lapkowski, J. Soloducho, K. Darowicki and A. P. Monkman, *Electrochim. Acta*, 2015, **184**, 86–93.
- S. Miyamoto, N. Miyake, L. F. Jarskog, W. W. Fleischhacker and J. A. Lieberman, *Mol. Psychiatry*, 2012, **17**, 1206–1227.
- F. B. Dias, T. J. Penfold and A. P. Monkman, *Methods Appl. Fluoresc.*, 2017, **5**, 12001.
- F. B. Dias, J. Santos, D. R. Graves, P. Data, R. S. Nobuyasu, M. A. Fox, A. S. Batsanov, T. Palmeira, M. N. Berberan-Santos, M. R. Bryce and A. P. Monkman, *Adv. Sci.*, 2016, **3**, 1600080.
- M. Okazaki, Y. Takeda, P. Data, P. Pander, H. Higginbotham, A. P. Monkman and S. Minakata, *Chem. Sci.*, 2017, **8**, 2677–2686.
- H. Tanaka, K. Shizu, H. Nakanotani and C. Adachi, *J. Phys. Chem. C*, 2014, **118**, 15985–15994.
- Z. Yang, Z. Mao, Z. Xie, Y. Zhang, S. Liu, J. Zhao, J. Xu, Z. Chi and M. P. Aldred, *Chem. Soc. Rev.*, 2017, **46**, 915–1016.
- A. Endo, M. Ogasawara, A. Takahashi, D. Yokoyama, Y. Kato and C. Adachi, *Adv. Mater.*, 2009, **21**, 4802–4806.
- H. Uoyama, K. Goushi, K. Shizu, H. Nomura and C. Adachi, *Nature*, 2012, **492**, 234–238.
- H. Kaji, H. Suzuki, T. Fukushima, K. Shizu, K. Suzuki, S. Kubo, T. Komino, H. Oiwa, F. Suzuki, A. Wakamiya, Y. Murata and C. Adachi, *Nat. Commun.*, 2015, **6**, 1–8.
- F. B. Dias, K. N. Bourdakos, V. Jankus, K. C. Moss, K. T. Kamtekar, V. Bhalla, J. Santos, M. R. Bryce and A. P. Monkman, *Adv. Mater.*, 2013, **25**, 3707–3714.
- M. K. Etherington, F. Franchello, J. Gibson, T. Northey, J. Santos, J. S. Ward, H. F. Higginbotham, P. Data, A. Kurowska, P. L. Dos Santos, D. R. Graves, A. S. Batsanov, F. B. Dias, M. R. Bryce, T. J. Penfold and A. P. Monkman, *Nat. Commun.*, 2017, **8**, 14987.
- R. Komatsu, H. Sasabe, Y. Seino, K. Nakao and J. Kido, *J. Mater. Chem. C*, 2016, **4**, 2274–2278.
- P. L. dos Santos, J. S. Ward, M. R. Bryce and A. P. Monkman, *J. Phys. Chem. Lett.*, 2016, **7**, 3341–3346.
- P. Data, P. Pander, M. Okazaki, Y. Takeda, S. Minakata and A. P. Monkman, *Angew. Chemie - Int. Ed.*, 2016, **55**, 5739–5744.
- M. N. Berberan-Santos and J. M. M. Garcia, *J. Am. Chem. Soc.*, 1996, **118**, 9391–9394.
- C. Baleizão and M. N. Berberan-Santos, *J. Chem. Phys.*, 2007, **126**, 204510.
- H. Higginbotham, K. Karon, P. Ledwon and P. Data, *Disp. Imaging*, 2017, **2**, 207–216.
- V. Jankus, P. Data, D. Graves, C. McGuinness, J. Santos, M. R. Bryce, F. B. Dias and A. P. Monkman, *Adv. Funct. Mater.*, 2014, **24**, 6178–6186.
- P. Data, R. Motyka, M. Lapkowski, J. Suwinski, S. Jursenas, G. Kreiza, A. Miasojedovas and A. P. Monkman, *Electrochim. Acta*, 2015, **182**, 524–528.
- C. A. Parker and C. G. Hatchard, *Trans. Faraday Soc.*, 1961, **57**, 1894.
- F. B. Dias, J. Santos, D. Graves, P. Data, R. S. Nobuyasu, M. A. Fox, A. S. Batsanov, T. Palmeira, M. N. Berberan-Santos, M. R. Bryce and A. P. Monkman, *Adv. Sci.*, 2016, **201600080**, 1–10.
- C. Adachi, M. A. Baldo, M. E. Thompson and S. R. Forrest, *J. Appl. Phys.*, 2001, **90**, 5048–5051.
- H. Yersin, *Top. Curr. Chem.*, 2004, 1–26.
- M. A. Baldo, D. F. O'Brien, Y. You, A. Shoustikov, S. Sibley, M. E. Thompson and S. R. Forrest, *Nature*, 1998, **395**, 151–154.

ARTICLE

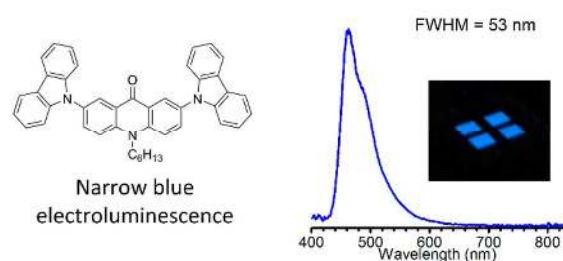
Journal Name

- 34 X.-L. Chen, C.-S. Lin, X.-Y. Wu, R. Yu, T. Teng, Q.-K. Zhang, Q. Zhang, W.-B. Yang and C.-Z. Lu, *J. Mater. Chem. C*, 2015, **3**, 1187–1195.
- 35 T. Hofbeck, U. Monkowius and H. Yersin, *J. Am. Chem. Soc.*, 2015, **137**, 399–404.
- 36 M. J. Leitl, V. A. Krylova, P. I. Djurovich, M. E. Thompson and H. Yersin, *J. Am. Chem. Soc.*, 2014, **136**, 16032–16038.
- 37 G. Li, R. S. Nobuyasu, B. Zhang, Y. Geng, B. Yao, Z. Xie, D. Zhu, G. Shan, W. Che, L. Yan, Z. Su, F. B. Dias and M. R. Bryce, *Chem. - A Eur. J.*, 2017, **23**, 11761–11766.
- 38 P. Pander, A. Swist, J. Soloducho and F. B. Dias, *Dye. Pigment.*, 2017, **142**, 315–322.
- 39 S. Mukherjee and P. Thilagar, *Chem. Commun.*, 2015, **51**, 10988–11003.
- 40 G. He, W. Torres Delgado, D. J. Schatz, C. Merten, A. Mohammadpour, L. Mayr, M. J. Ferguson, R. McDonald, A. Brown, K. Shankar and E. Rivard, *Angew. Chemie - Int. Ed.*, 2014, **53**, 4587–4591.
- 41 S. Hirata, K. Totani, J. Zhang, T. Yamashita, H. Kaji, S. R. Marder, T. Watanabe and C. Adachi, *Adv. Funct. Mater.*, 2013, **23**, 3386–3397.
- 42 Y. Gong, G. Chen, Q. Peng, W. Z. Yuan, Y. Xie, S. Li, Y. Zhang and B. Z. Tang, *Adv. Mater.*, 2015, **27**, 6195–6201.
- 43 B. K. Sharma, A. M. Shaikh, N. Agarwal and R. M. Kamble, *RSC Adv.*, 2016, **6**, 17129–17137.
- 44 P. Pander, A. Swist, P. Zassowski, J. Soloducho, M. Lapkowski and P. Data, *Electrochim. Acta*, 2017, **257**, 192–202.
- 45 M. Y. Wong, M.-G. La-Placa, A. Pertegas, H. J. Bolink and E. Zysman-Colman, *J. Mater. Chem. C*, 2017, **5**, 1699–1705.
- 46 T. Serevičius, T. Nakagawa, M. Kuo, S. Cheng, K.-T. Wong, C.-H. Chang, R. C. Kwong, S. Xia and C. Adachi, *Phys. Chem. Chem. Phys.*, 2013, **15**, 15850.
- 47 M. Kim, S. K. Jeon, S. Hwang and J. Y. Lee, *Adv. Mater.*, 2015, **27**, 2515–2520.
- 48 J. Lee, K. Shizu, H. Tanaka, H. Nomura, T. Yasuda and C. Adachi, *J. Mater. Chem. C*, 2013, **1**, 4599.
- 49 D. R. Lee, M. Kim, S. K. Jeon, S. Hwang, C. W. Lee and J. Y. Lee, *Adv. Mater.*, 2015, **27**, 5861–5867.
- 50 T. Hatakeyama, K. Shiren, K. Nakajima, S. Nomura, S. Nakatsuka, K. Kinoshita, J. Ni, Y. Ono and T. Ikuta, *Adv. Mater.*, 2016, **28**, 2777–2781.
- 51 M. K. Etherington, J. Gibson, H. F. Higginbotham, T. J. Penfold and A. P. Monkman, *Nat. Commun.*, 2016, **7**, 13680.
- 52 P. L. dos Santos, J. S. Ward, A. S. Batsanov, M. R. Bryce and A. P. Monkman, *J. Phys. Chem. C*, 2017, **121**, 16462–16469.
- 53 H. Tanaka, K. Shizu, H. Nakanotani and C. Adachi, *J. Phys. Chem. C*, 2014, **118**, 15985–15994.
- 54 S. T. Hoffmann, P. Schrögel, M. Rothmann, R. Q. Albuquerque, P. Strohriegel and A. Köhler, *J. Phys. Chem. B*, 2011, **115**, 414–421.
- 55 M. C. Castex, C. Olivero, G. Pichler, D. Adès and A. Siove, *Synth. Met.*, 2006, **156**, 699–704.
- 56 J. Li, Q. Zhang, H. Nomura, H. Miyazaki and C. Adachi, *Appl. Phys. Lett.*, 2014, **105**, 13301.
- 57 R. Huang, J. Avó, T. Northey, E. Channing-Pearce, P. L. dos Santos, J. S. Ward, P. Data, M. K. Etherington, M. A. Fox, T. J. Penfold, M. N. Berberan-Santos, J. C. Lima, M. R. Bryce and F. B. Dias, *J. Mater. Chem. C*, 2017, **5**, 6269–6280.
- 58 C. Baleizão and M. N. Berberan-Santos, *ChemPhysChem*, 2011, **12**, 1247–1250.
- 59 J. S. Ward, R. S. Nobuyasu, A. S. Batsanov, P. Data, A. P. Monkman, F. B. Dias and M. R. Bryce, *Chem. Commun.*, 2016, **52**, 3–6.
- 60 R. Pashazadeh, P. Pander, A. Lazauskas, F. B. Dias and J. V. Grazulevicius, *J. Phys. Chem. Lett.*, 2018, **9**, 1172–1177.

View Article Online
DOI: 10.1039/C8TC00175H

Thermally Activated Delayed Fluorescence with Narrow Emission Spectrum and Organic Room Temperature Phosphorescence by Controlling Spin-Orbit Coupling and Phosphorescence Lifetime of Metal-Free Organic Molecules

Piotr Pander, Agnieszka Swist, Radoslaw Motyka, Jadwiga Soloducho, Fernando B. Dias, Przemyslaw Data*



Novel acridone derivative is presented showing TADF and narrow blue electroluminescence.